Transactions of the VŠB – Technical University of Ostrava, Mechanical Series
No. 1, 2014, vol. LX
article No.1977

Jana JABLONSKÁ[*], Jiří KUKELKA[**], Matěj PETROVIČ[***]

FLOW IN THE NON-RETURN FLAP

PROUDĚNÍ VE ZPĚTNÉ KLAPCE

Abstract

The essay concerns issues connected with modelling of flow in a non-return flap and determination of force effects on the flap disc. The task was researched in collaboration with ARMATURY Group, a.s. The flow is non-compressible and the flow medium is water. Boundary conditions determined by a measurement were applied in the modelling. The target of the project is finding a suitable mathematical model and comparison of the measured and calculated values dissipation factor of the non-return flap for various opening angles of the flap disc.

Abstrakt

Článek se věnuje problematice modelování proudění ve zpětné klapce a určení silových účinků na klapku. Úloha je řešena ve spolupráci s firmou ARMATURY Group, a.s. Proudění je nestlačitelné a proudící medium je voda. Pro modelování jsou použity okrajové podmínky určené měřením. Cílem je určit vhodný matematický model a srovnat naměřené a vypočtené hodnoty ztrátového součinitele zpětné klapky pro různé úhly otevření talíře klapky.

Keywords

Loss coefficient, the pressure loss, check valves, mathematical model, Fluent

1 INTRODUCTION

The flow in the non-return flap is examined by means of a numerical model. The tool used in the numerical modelling is the Fluent program, which allows research on the flow in various geometries.

The basic physical laws describing the flow, such as a law of conservation of the momentum, the weight, heat or other scalar values, are described by Navier-Stokes equations together with the continuity equation, both for stationary and non-stationary flow. In case of non-stationary, non-compressible and non-isothermal flows, they have the following form [1, 2, 4]:

The continuity equation

$$\frac{\partial u}{\partial x}+\frac{\partial v}{\partial y}+\frac{\partial w}{\partial z}=0 \qquad (1)$$

[*] Ing., Ph.D., Department of hydromechanics and hydraulic equipment, Faculty of Mechanical Engineering, VŠB-Technical University of Ostrava, 17. listopadu 15/2171, 708 33 Ostrava – Poruba, Czech Republic, tel. (+420) 59 732 4269, e-mail jana.jablonska@vsb.cz

[**] Ing., Department of hydromechanics and hydraulic equipment, Faculty of Mechanical Engineering, VŠB-Technical University of Ostrava, 17. listopadu 15/2171, 708 33 Ostrava – Poruba, Czech Republic, tel. (+420) 59 732 4269, e-mail jiri.kukelka@vsb.cz

[***] Ing., Department of hydromechanics and hydraulic equipment, Faculty of Mechanical Engineering, VŠB-Technical University of Ostrava, 17. listopadu 15/2171, 708 33 Ostrava – Poruba, Czech Republic, tel. (+420) 59 732 4269, e-mail matej.petrovic21@gmail.com

where:

u, v, w – components of the velocity,

Navier-Stokes equations

$$\frac{\partial u}{\partial t}+\frac{\partial(uu)}{\partial x}+\frac{\partial(uv)}{\partial y}+\frac{\partial(uw)}{\partial z}=\frac{1}{\rho}\frac{\partial p}{\partial x}+\nu\left(\frac{\partial^2 u}{\partial x^2}+\frac{\partial^2 u}{\partial y^2}+\frac{\partial^2 u}{\partial z^2}+\right)+f_x$$

$$\frac{\partial v}{\partial t}+\frac{\partial(vu)}{\partial x}+\frac{\partial(vv)}{\partial y}+\frac{\partial(vw)}{\partial z}=\frac{1}{\rho}\frac{\partial p}{\partial y}+\nu\left(\frac{\partial^2 v}{\partial x^2}+\frac{\partial^2 v}{\partial y^2}+\frac{\partial^2 v}{\partial z^2}+\right)+f_y \qquad (2)$$

$$\frac{\partial w}{\partial t}+\frac{\partial(wu)}{\partial x}+\frac{\partial(wv)}{\partial y}+\frac{\partial(ww)}{\partial z}=\frac{1}{\rho}\frac{\partial p}{\partial z}+\nu\left(\frac{\partial^2 w}{\partial x^2}+\frac{\partial^2 w}{\partial y^2}+\frac{\partial^2 w}{\partial z^2}+\right)+f_z$$

where:

u, v, w – components of the velocity,

ρ – density,

ν – kinematic viscosity,

p – pressure,

f_x, f_y, f_z – components of external body forces.

1.1 Finite volume method

The method is based on division of an area to discrete volumes given by a calculation grid, balancing of unknown values in the individual finite values and numerical solution of discretized equations.

1.2 Standard two-equation $k-\varepsilon$ model

When deriving the model, it is presumed that the turbulent flow is fully deployed and effects of molecular viscosity are negligible.

Transparent equation

$$\frac{\partial(\rho k)}{\partial t}+\frac{\partial(\rho u_i k)}{\partial x_i}=\frac{\partial}{\partial x_j}\left[\left(\mu+\frac{\mu_t}{\sigma_k}\right).\frac{\partial k}{\partial x_j}\right]+G_k+G_b-\rho\varepsilon-Y_M+S_k \qquad (3)$$

$$\frac{\partial(\rho\varepsilon)}{\partial t}+\frac{\partial(\rho u_i \varepsilon)}{\partial x_i}=\frac{\partial}{\partial x_j}\left[\left(\mu+\frac{\mu_t}{\sigma_\varepsilon}\right).\frac{\partial \varepsilon}{\partial x_j}\right]+C_{1\varepsilon}\frac{\varepsilon}{k}\left(G_k+C_{3\varepsilon}G_b\right)-C_{2\varepsilon}\rho\frac{\varepsilon^2}{k}+S_\varepsilon \qquad (4)$$

where:

G_k – represents turbulent kinetic energy related to the medium velocity,

G_b – represents turbulent kinetic energy related to the buoyancy,

Y_M – represents growth of fluctuating dilatation into compressible turbulence related to the total dissipation output,

S_k and S_ε – defined constants,

$C_{1\varepsilon}$, $C_{2\varepsilon}$, $C_{3\varepsilon}$ – constants $C_{1\varepsilon}=1{,}44$; $C_{2\varepsilon}=1{,}92$;

σ_k, σ_ε – Prandtl turbulence numbers defined for k and ε, $\sigma_k=1$; $\sigma_\varepsilon=1{,}3$.

Turbulent kinetic energy related to the medium velocity

$$G_k = \mu_t S^2 = \mu_t \left(\sqrt{2 S_{ij} S_{ij}} \right)^2 \tag{5}$$

where:

S – tensor of medium velocity module deformation.

Generation of the turbulence as a result of the upward lift is given

$$G_b = \beta g_i \frac{\mu_t}{\mathrm{Pr}_t} \frac{\partial T}{\partial x_i}^2 \tag{6}$$

where:

Pr_t – is a turbulent Prandtl number of energy,

g_i – is the i-fold component of the gravitational vector,

β – thermal expansion coefficient.

Effect of compressibility on the turbulences

$$Y_M = 2 \rho \varepsilon M_t^2 \tag{7}$$

where:

M_t – turbulent Mach number.

$$M_t = \sqrt{\frac{k}{a^2}} \tag{8}$$

where:

a – velocity of sound in the liquid.

Turbulent viscosity is defined

$$\mu_t = \rho C_\mu \frac{k^2}{\varepsilon} \tag{9}$$

where:

C_μ – constant, $C_\mu = 0{,}09$. [1, 2, 4]

1.3 Standard $k-\omega$ model

The standard $k-\omega$ model in the FLUENT program is based on Wilcox $k-\omega$ model, which adds modifications for low Reynolds numbers, compressibility and distribution of shear stress. The standard $k-\omega$ model is an empiric model based on transport equations for turbulent kinetic energy k and a specific proportion of dissipation ω, which can be understood as a proportion of ω to k.

During years-lasting modifications of the $k-\omega$ model, conditions were added to the equations for k and ω, which improved accuracy of the model in prediction of shear stress.

Transport equation for the $k-\omega$ model

Turbulent kinetic energy k and specific proportion of dissipation ω are obtained from the following transport equations [1, 2]

$$\frac{\partial}{\partial t}(\rho k) + \frac{\partial}{\partial x_i}(\rho u_i k) = \frac{\partial}{\partial x_j}\left(\Gamma_k \frac{\partial k}{\partial x_j} \right) + G_k - Y_k + S_k \tag{10}$$

$$\frac{\partial}{\partial t}(\rho\omega)+\frac{\partial}{\partial x_i}(\rho u_i\omega)=\frac{\partial}{\partial x_j}\left(\Gamma_\omega\frac{\partial\omega}{\partial x_j}\right)+G_\omega-Y_\omega+S_\omega \tag{11}$$

where:

G_k – production of turbulent kinetic energy as a result of the medium velocity gradient,

G_ω – production of ω,

Γ_k, Γ_ω – effective diffusivity k and ω,

Y_k, Y_ω – dissipation k and ω as a result of turbulence,

S_k, S_ω – source term defined by the user.

Effective dissipation for $k-\omega$ is specified as follows [1]

$$\Gamma_k=\mu+\frac{\mu_t}{\sigma_k} \tag{12}$$

$$\Gamma_\omega=\mu+\frac{\mu_t}{\sigma_\omega} \tag{13}$$

where:

σ_k, σ_ω – turbulent Prandtl numbers for k and ω,

μ_t – turbulent viscosity.

Literature defines turbulent viscosity as [1]

$$\mu_t=\alpha^*\frac{\rho k}{\omega} \tag{14}$$

Coefficient α^* incorporates corrections for low Reynolds numbers and is defined as [1]

$$\alpha^*=\alpha_\infty^*\left(\frac{\alpha_0^*+\mathrm{Re}_t/R_k}{1+\mathrm{Re}_t/R_k}\right) \tag{15}$$

where:

$$\mathrm{Re}_t=\frac{\rho k}{\mu\omega} \tag{16}$$

$$\alpha_0^*=\frac{\beta_i}{3} \tag{17}$$

$R_k=6$; $\beta_i=0{,}072$

It applies to high Reynolds numbers

$$\alpha^*=\alpha_\infty^*=1 \tag{18}$$

2 MODELLED NON-RETURN EXTRACTION FLAP

2.1 Computation grid

The piping with the flap is modelled as a 3D body; the length of the inlet pipe is 270 mm. The used dimensions followed the instruction. As the goal concerns a flow analysis behind the flap, the output pipe is longer.

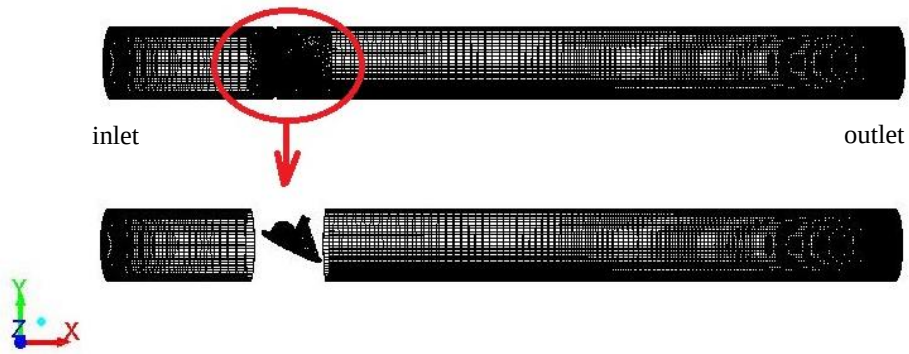

Fig. 1 3D geometry - grid

Each flap position had to be resolved as a new task. This is why the individual tasks have different numbers of cells. The number of cells slightly rises with the rising opening angle of the flap.

2.2 Definition of boundary conditions and setting parameters for the solution

The boundary conditions were delivered by ARMATURY Group, a.s., which performed measurements on the modelled valve. The PRESSURE INLET condition was used on the inlet, because the total or static pressure is known. Next, the flow (mass or volume flow) or the velocity must be known. This condition is also suitable for the flow when buoyancy forces are considered. The total relative pressure is defined on the inlet and is related to the operating pressure by a relation derived from Bernoulli's equation while the density is constant or is the function of the temperature [1, 2, 3, 5, 6].

The MASS-FLOW condition, which is used for non-compressible flow, was defined on the outlet. The compressible flow assumes non-constant density, which depends on the state values of pressure and temperature and affects the volume flow and thus the velocity, which can lead to wrong results. This condition and its dependency can be defined by means of the volume flow equation. Where ρ represents density of the flowing liquid, S is the area of the section and v is the speed of the liquid flow. [1, 2, 3, 5, 6]

$$Q_m = \rho Q = \rho S v \tag{19}$$

As regards adjustment of the input boundary condition, the turbulent parameters have a great significance as values of turbulent kinetic energy and dissipation. A constant value estimated by experience can be present. These turbulence values can also be determined by means of more easily determinable values such as the intensity of turbulence, proportion between the turbulent and molecule viscosity, the hydraulic diameter and the length-scale of the turbulence. [1, 2]

Tab. 1 Boundary conditions

inlet	PRESSURE INLET	500000 Pa
outlet	MAAS FLOW INLET	mass flow rate Q_m [kg.s^{-1}]

Physical properties of water as the flow medium are density 998.2 kg.m^{-3} and dynamic viscosity is 0.001003 Pa.s. The properties are constant. The temperature of the flowing water is 20 °C.

3 RESULTS OF THE MODELLING

3.1 Comparison of the models

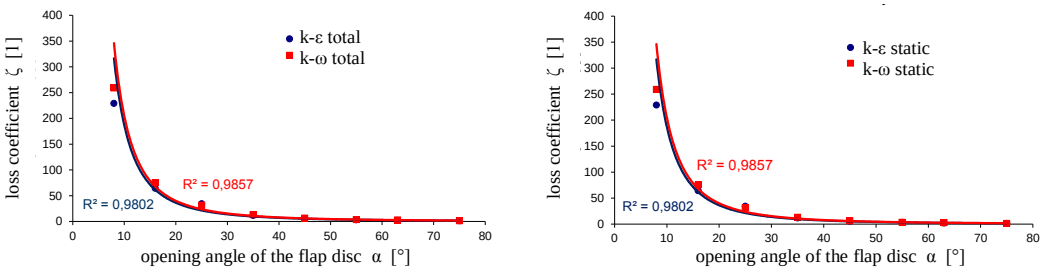

total pressure static pressure

Fig. 2 Comparison of the methods

3.2 Drag coefficient

Speed determination

$$Q_v = Sv = \frac{\pi d^2}{4} c \qquad \Rightarrow \qquad c = \frac{4Q_v}{\pi d^2}$$

Reynolds number

$$\mathrm{Re} = \frac{cd}{\upsilon}$$

where:

d – piping diameter [m],

υ – kinematic viscosity [$m^2.s^{-1}$].

Dissipation factor

$$\xi = \frac{2\Delta p_z}{\rho c^2}$$

Flow rate coefficient [3, 5, 6]

$$K_v = q_v \sqrt{\frac{\rho}{\Delta p_z \rho_0}}$$

where:

q_v – flow [$m^3.h^{-1}$],

ρ – water density [$kg.m^{-3}$],

ρ_0 – water density at 15°C [$kg.m^{-3}$],

Δp_z – pressure loss of the fixtures [bar].

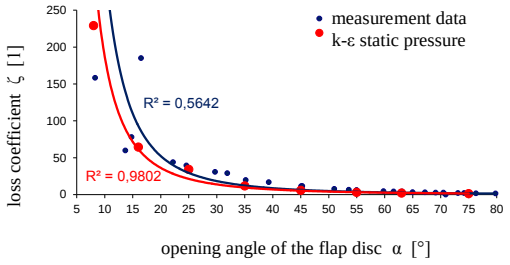

standard k-ε model, static pressure

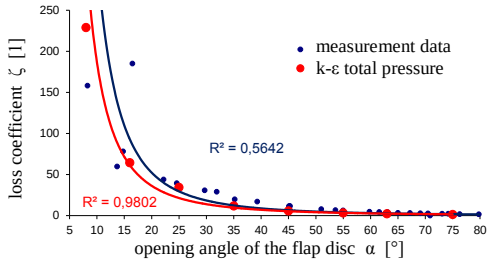

standard k-ε model, total pressure

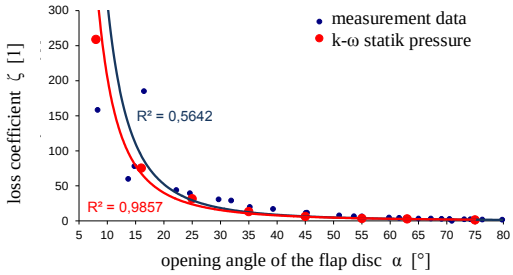

standard k–ω model, static pressure

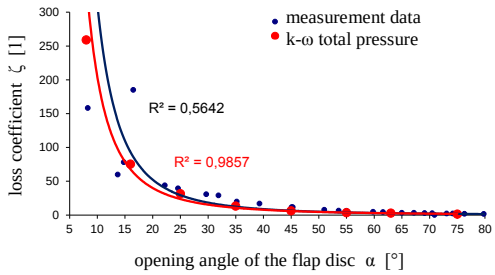

standard k– ω model, total pressure

Fig. 3 Dependency of the dissipation factor on the opening angle of the flap disc

scale	minimum 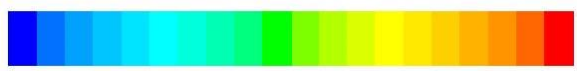 maximum
angle	contours of the pressure / range
8	
	(461363 - 500003) Pa
25	
	(480423 - 500560) Pa
45	
	(483859 - 500163) Pa
55	
	(481909 - 500350) Pa
75	
	(447052 - 501794) Pa

Fig. 4 Contours of the pressure

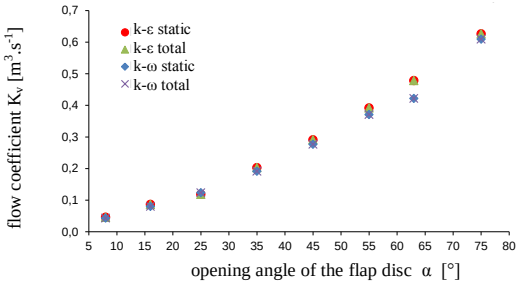

Fig. 5 Dependency of the flow factor on the opening angle of the flap disc

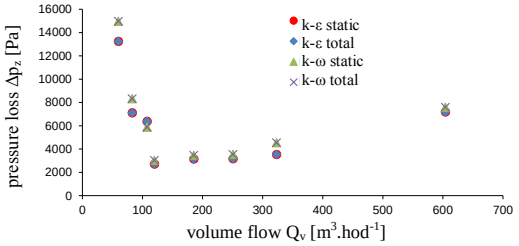

Fig. 6 Dependency of pressure loss on the volume flow

3.3 Forces on the flap disc

Tab. 1 Forces affecting the flap disc

angle	F_x	F_y	F_z	F_{xy}	F_{xyz}	δF
[°]	[N]	[N]	[N]	[N]	[N]	[%]
8	755,1	558,3	-1,80	939,027	939,029	1,84E-04
25	242,5	402,4	0,02	469,821	469,821	-9,06E-08
45	115,2	391,0	-0,07	407,618	407,618	-1,47E-06
55	107,0	402,5	-0,15	416,480	416,480	-6,49E-06
75	172,5	426,2	-3,40	459,786	459,798	-2,73E-03

Resulting force x, y

$$F_{x,y} = \sqrt{F_x^2 + F_y^2}$$

Resulting force x, y, z [5, 6]

$$F_{x,y,z} = \sqrt{F_x^2 + F_y^2 + F_z^2}$$

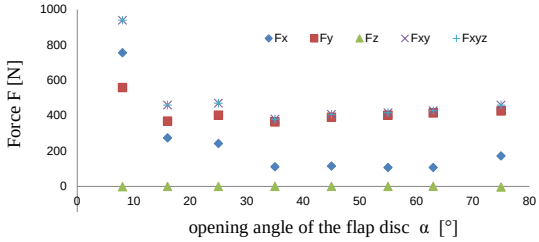

Fig. 7 Dependence of the force on the opening angle of the flap disc

4 CONCLUSIONS

The non-return extraction flap was solved as a 3D task in the Fluent CFD code. The flow was modelled as stationary. The medium was water with constant properties (non-compressible).

Several options of the flap disc opening were solved and it became evident that the number of cells was rising with the increasing opening angle, but the number of iteration was dropping. The drop of iteration is caused by a more steady flow (it is depended on formation of vortex regions behind the flap).

It is evident from Fig. 2 that the differences in evaluation of the dissipation factor from the total or static pressure are negligible. The dynamic pressure has no impact on the dissipation factor. This can be documented by a chart in Fig. 5 - dependency of the flow coefficient on the opening angle of the flap.

It is suitable to use boundary conditions from the measured values: input – pressure, output volume flow.

Two turbulence models were used in the solution - k-ε model and k– ω model. In Fig. 3 Dependency of the dissipation factor on the opening angle of the flap disc, dissipation factors of both models are evaluated in relation to the opening angle of the flap, which shows that the differences are minimal. In addition, the given illustration compares the individual models with the measured values. If the opening angles of the flap are larger, the measured and calculated values are identical, but there are differences in angles smaller than 35°. Discrepancy of these values can be caused by accuracy of the measurement because the measurement results at smaller angles are not definite.

The contours of the pressure for different opening angle of the flap disc are evaluated in Fig. 4 - contours of the pressure.

A force affecting the flap where the z-component can be neglected was also evaluated. It is evident from Fig. 7 that the lowest force acts when the non-return extract flap is open at the angle of 35°. As the flap is being closed, the force is growing parabolically, if it is open more than 35°, the force grows only slightly.

Modelling of the non-return extraction flap can continue with steam as the medium and the flow will be compressible. The precondition, however, is setting of real boundary conditions.

ACKNOWLEDGEMENTS

This paper has been elaborated in the framework of the project Opportunity for young researchers, reg. no. CZ.1.07/2.3.00/30.0016, supported by Operational Programme Education for Competitiveness and co-financed by the European Social Fund and the state budget of the Czech Republic.

The article was written in collaboration with the ARMATURY Group Company, which contributed with its professional expertise and measurements in creation of this publication.

REFERENCES

[1] FLUENT: FLUENT 12 - *User's guide.* Fluent Inc. 2007 [online]. Dostupné z < http://spc.vsb.cz/portal/cz/documentation/manual/index.php >.

[2] KOZUBKOVÁ, M. Modelování proudění tekutin FLUENT, CFX, VŠB-TU Ostrava, 2008. [online]. Datum poslední revize12.12.2008. Dostupné z < http://www.338.vsb.cz/PDF/Kozubkova-Fluent.pdf >

[3] CHAMIEH, D. S., ACOSTA, A. J., BRENNEN, C. E., CAUGHEY, T. K. *Experimental Measurements of Hydrodynamic Radial Forces and Stiffness Matricesfor a Centrifugal Pump-Impeller*. [online], Datum poslední revise 13.5.2004. Dostupné z< http://authors.library.caltech.edu/81/1/CHA064.pdf>.

[4] KOZUBKOVÁ, M. *Modelování proudění - Fluent I.* VŠB-TU Ostrava, 2008. 154s. Dostupné z < http://www.338.vsb.cz/studium9.htm >

[5] ROČEK, J. Závěrečná zpráva o měření zpětných klapek DN 100 a DN 250. 31s.

[6] ČSN EN 1267 Průmyslové armatury – Měření průtokových ztrát s použitím vody jako zkušební tekutiny. Srpen 2012.